NASA / CR-1998-208454

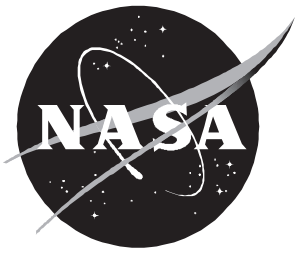

A Study of Failure in Small Pressurized Cylindrical Shells Containing a Crack

Craig A. Barwell, Lorenz Eber, and Ian M. Fyfe
University of Washington, Seattle, Washington

August 1998

The NASA STI Program Office . . . in Profile

Since its founding, NASA has been dedicated to the advancement of aeronautics and space science. The NASA Scientific and Technical Information (STI) Program Office plays a key part in helping NASA maintain this important role.

The NASA STI Program Office is operated by Langley Research Center, the lead center for NASA's scientific and technical information. The NASA STI Program Office provides access to the NASA STI Database, the largest collection of aeronautical and space science STI in the world. The Program Office is also NASA's institutional mechanism for disseminating the results of its research and development activities. These results are published by NASA in the NASA STI Report Series, which includes the following report types:

- TECHNICAL PUBLICATION. Reports of completed research or a major significant phase of research that present the results of NASA programs and include extensive data or theoretical analysis. Includes compilations of significant scientific and technical data and information deemed to be of continuing reference value. NASA counter-part or peer-reviewed formal professional papers, but having less stringent limitations on manuscript length and extent of graphic presentations.

- TECHNICAL MEMORANDUM. Scientific and technical findings that are preliminary or of specialized interest, e.g., quick release reports, working papers, and bibliographies that contain minimal annotation. Does not contain extensive analysis.

- CONTRACTOR REPORT. Scientific and technical findings by NASA-sponsored contractors and grantees.

- CONFERENCE PUBLICATION. Collected papers from scientific and technical conferences, symposia, seminars, or other meetings sponsored or co-sponsored by NASA.

- SPECIAL PUBLICATION. Scientific, technical, or historical information from NASA programs, projects, and missions, often concerned with subjects having substantial public interest.

- TECHNICAL TRANSLATION. English-language translations of foreign scientific and technical material pertinent to NASA's mission.

Specialized services that help round out the STI Program Office's diverse offerings include creating custom thesauri, building customized databases, organizing and publishing research results . . . even providing videos.

For more information about the NASA STI Program Office, see the following:

- Access the NASA STI Program Home Page at ***http://www.sti.nasa.gov***

- Email your question via the Internet to help@sti.nasa.gov

- Fax your question to the NASA Access Help Desk at (301) 621-0134

- Phone the NASA Access Help Desk at (301) 621-0390

- Write to:
  NASA Access Help Desk
  NASA Center for AeroSpace Information
  7121 Standard Drive
  Hanover, MD 21076-1320

NASA / CR-1998-208454

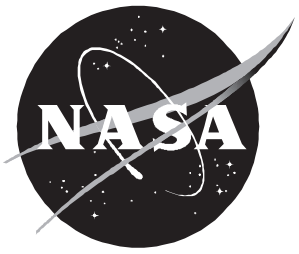

A Study of Failure in Small Pressurized Cylindrical Shells Containing a Crack

Craig A. Barwell, Lorenz Eber, and Ian M. Fyfe
University of Washington, Seattle, Washington

National Aeronautics and
Space Administration

Langley Research Center
Hampton, Virginia 23681-2199

Prepared for Langley Research Center
under Grant NAG1-1586

August 1998

Available from the following:

NASA Center for AeroSpace Information (CASI)
7121 Standard Drive
Hanover, MD 21076-1320
(301) 621-0390

National Technical Information Service (NTIS)
5285 Port Royal Road
Springfield, VA 22161-2171
(703) 487-4650

TABLE OF CONTENTS

	PAGE
SUMMARY	1
INTRODUCTION	2
APPARATUS AND PROCEDURES	4
Experimental Equipment	4
Instrumentation	4
Specimen Configuration	6
Computational Aspects	7
RESULTS	9
Bulge Deformations	9
Axial and Hoop Strains	11
Crack Opening Displacements	14
Crack Tip Opening Angle (C.T.O.A.)	16
Unsymmetric Loading	20
CONCLUDING REMARKS	24
REFERENCES	26
APPENDIX	28

A STUDY OF FAILURE IN SMALL PRESSURIZED CYLINDRICAL SHELLS CONTAINING A CRACK

Craig A. Barwell, Lorenz Eber & Ian M. Fyfe,

Department of Aeronautics & Astronautics
University of Washington

SUMMARY

The deformation in the vicinity of axial cracks in thin pressurized cylinders is examined using small experimental models. The loading applied was either symmetric or unsymmetric about the crack plane, the latter being caused by structural constraints such as stringers. The objective was twofold - one, to provide the experiment results which will allow computer modeling techniques to be evaluated for deformations that are significantly different from that experienced by flat plates, and the other to examine the deformations and conditions associated with the onset of crack kinking which often precedes crack curving.

The stresses which control crack growth in a cylindrical geometry depend on conditions introduced by the axial bulging, which is an integral part of this type of failure. For the symmetric geometry, both the hoop and radial strain just ahead of the crack, r = a, were measured and these results compared with those obtained from a variety of structural analysis codes, in particular STAGS [1], ABAQUS and ANSYS. In addition to these measurements, the pressures at the onset of stable and unstable crack growth were obtained, and the corresponding crack deformations measured as the pressures were increased to failure. For the unsymmetric cases, measurements were taken of the crack kinking angle and the displacements in the vicinity of the crack.

In general, the strains ahead of the crack showed good agreement between the three computer codes, and between the codes and the experiments. In the case of crack behavior, it was determined that modeling stable tearing with a crack-tip opening displacement fracture criterion could be successfully combined with the finite-element analysis techniques as used in structural analysis codes. The analytic results obtained in this study were very compatible with the experimental observations of crack growth. Measured crack kinking angles also showed good agreement with theories based on the maximum principle stress criterion.

INTRODUCTION

When a crack curves sufficiently to allow the internal pressure to cause a shell to open in a small area we have a condition in which controlled decompression occurs by flapping [2]. However, although crack growth to a flapped condition is very desirable, the techniques to model this type of crack growth are still being developed, and so the experimental data to verify these models is also required. The research described in this report examines crack growth in thin cylinders under conditions that produce the deformations that are unique to constrained thin cylinders.

It has been known for some time that bulging [3,4], which occurs when a pressurized cylinder has a longitudinal crack, plays an important role in crack growth. In addition to the bulge if the loading is unsymmetric, due to the presence of a stringer or other constraint, the resultant mode II deformations result in a crack whose growth is along a curved path. This turning, together with the presence of a constraint, introduces a tearing, or "nominal mode-III" type of loading. This latter effect could be important in fuselage failure, and is so recognized in the recent work by Ingraffea and associates [5,6]. Although experimental research in this area has been quite limited, an important study on a full scale fuselage is described by Miller et al [7]. However, because of the high costs involved in full scale studies the use of small or sub-scale cylindrical models provides an attractive alternative as a means of obtaining the required data.

Tests in thin walled cylinders pose unique problems in that a pressurized cylinder is expected to have a sizable leak before the fatigue crack has propagated any significant distance. In an aircraft fuselage, where the pressure is quite low, two conditions exist which could allow significant undetected crack growth, these being that air loss is reduced because of insulating blankets, and minor air loss can be compensated for by the air conditioning system. In thin cylinders when the crack curves, the internal pressure is then acting on a flap, and so the loading for the "nominal mode III" increases. These complications require extensive testing of any proposed models, and so the need for sub scale testing also increases if costs are to be contained. An example of sub-scale testing is shown in Fig. 1, where fatigue crack growth next to a stringer in a pressurized thin cylinder shows the effect of unsymmetric loading on the crack path. In this case the cylinder is only 2.5 inches in diameter, but the crack behavior is almost identical to that described in [7].

In using scale models one usually hopes that not only is the model geometrically similar, but also has complete similarity. However, with the small radius of the cylinders used in this study, geometric similarity would require the cylinder model to have a thickness so small that this requirement can not be met. It is this lack of geometric similarity that suggests the use of sub-scale to describe the type of model being studied.

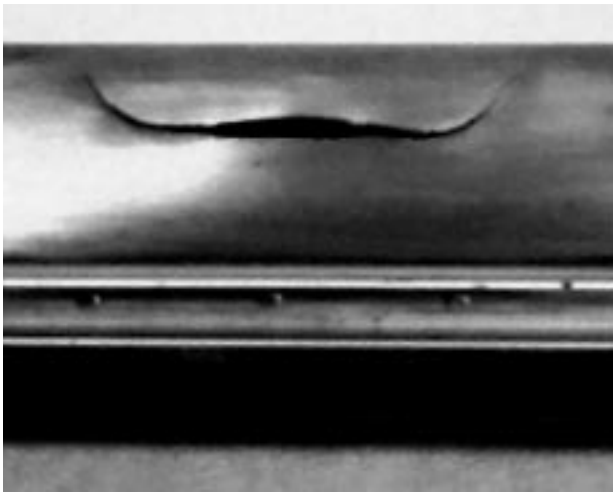

Fig. 1 An Unsymmetric Fatigue Crack near a Stringer in a 2.5 ins. Diameter Thin Cylindrical Shell

APPARATUS AND PROCEDURES

Experimental Apparatus

The hydraulic system used in this project was designed to apply a variety of loads to the cylinders, such as, montonically increasing static pressure, axial loads and cyclic internal pressures. Depending on the type of tests being carried out, either oil or water could be used as the hydraulic fluid. In this particular project water was used in all the tests, and the axial and cyclic loading features were disconnected. A drawing of this system is shown in Fig. 2a

Two problems that apply in particular to thin cylinder testing are, the conditions introduced by the need to close the ends of the cylinder, and the method required to seal any existing cracks. In this study, the former was handled by specially designed end plates, shown in Fig. 2b, in which the specimen is supported by two holding plates which are used to transfer the axial loading caused by internal pressure to external supports, so that the axial load is independent of the internal pressure. This resulted in a cylinder loaded so that the axial stresses some distance from the crack were zero, that this condition was satisfied was checked from strain data obtained from gauges placed close to the ends of the cylinders. In addition to checking this particular end condition, this data was also used to show that the results obtained were compatible with the theory associated with infinitely long cylinders, and was also in accord with the values obtained from the STAGS finite element code. To prevent leakage through the crack during the tests, a metallized polyester tape (3M "Scotchtab") was used. This tape is only 0.002 inches thick, and has a Young's modulus of approximately one tenth that of aluminum. The strip was pleated to allow tangential expansion, as shown in Fig. 2c. The strip was attached to the cylinder by its pressure sensitive adhesive backing, but silicone grease was applied in the region of the crack to allow free movement of this seal.

Instrumentation

In addition to the pressure as the specimen was loaded to failure, a number of additional measurements were taken. In particular, strains ahead of the crack tip, crack opening displacement at the midpoint of the crack (C.M.O.D.), the crack tip opening angle (C.T.O.A.), radial displacements along the crack faces and ahead of the crack tip, and the length of stable crack growth before catastrophic failure.

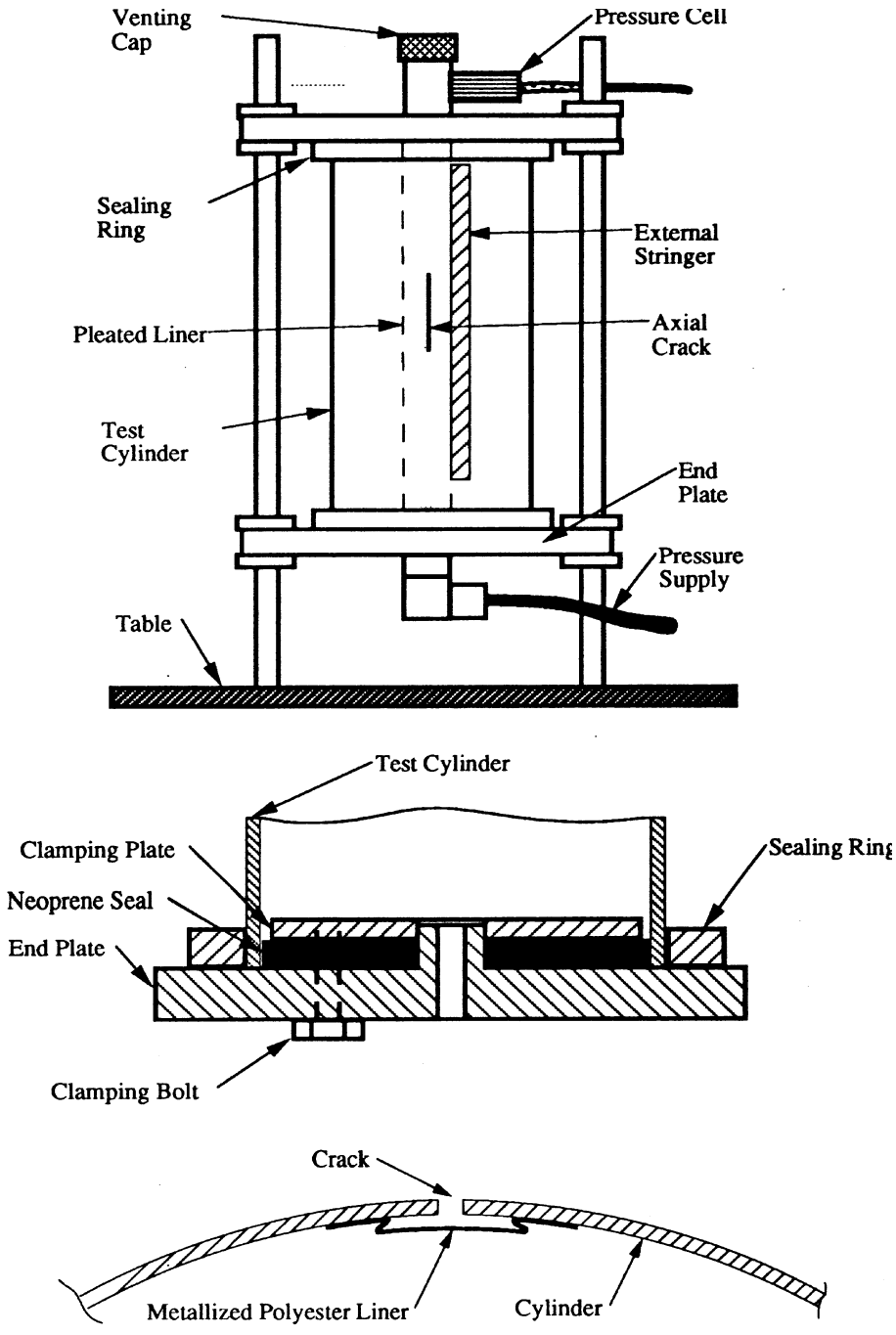

Fig. 2 Experimental Configuration for Thin Cylinder Testing

Strains were measured using standard metal foil electrical resistance strain gauges, which were located near the crack tip (at r = a) in the plane of the crack, and also near the ends of the specimens to confirm that the boundary conditions at the ends were satisfied. In cases where the loading was unsymmetric due to the presence of a stringer a strain gauge was located at the center of the crack in order to obtain the axial strains due to the bulge.

The crack opening displacement was measured using a standard clip gauge. The clip gauge arms had tabs machined onto the ends to allow insertion into a small hole drilled at the crack midpoint. Although this instrument was calibrated with a micrometer, allowance had to be made for a slight displacement caused by the crack seal pressing against the tabs when the pressure was first applied

With the introduction of the crack growth option to STAGS (version 2.3) it was also possible to compare the analysis predictions with data obtained from photographs of the deformation and growth of the crack prior to complete failure. Using a standard 35mm camera with a 60 mm AF Nicon micro lens and a Vivitar 2X macro focusing teleconverter it was also possible to determine the pressure at the onset of stable crack growth, the length of this growth before failure and the C.T.O.A. values.

Radial displacements were measured using a dial gauge, which was mounted horizontally, and suspended from two steel rods. The rods were in turn attached to a swing arm which pivoted about the venting cap at the top of the specimen. The rods could be moved vertically independent of the swing arm position, and thus allowed radial measurements to be taken over a fair portion of the cylinder around the crack. Although the dial gauge could measure to the nearest 0.0001 inches, the overall accuracy was much less, due to the slight play inherent in such a device.

Specimen Configuration

Three materials 2024-T3, 2024-O and 6061-T4 aluminum were used throughout the project. The 6061-T4 material, a standard stock tubing of 2.5-inch diameter with a wall thickness of 0.028 inches, was used in a series of preliminary tests to develop the required techniques, and to calibrate the system. These results will not be reported. The remaining specimens were manufactured from 2024-T3 and 2024-O clad sheet stock, with the latter material introduced to provide a low yield material that would emphasis the nonlinear and plasticity aspects of the deformations.

To eliminate end effects around the crack the specimen lengths were varied from 15 inches for the 6061-T4 specimens to 27.25 for the larger diameter 2024 specimens. The crack itself was actually a 0.020-inch wide slot cut axially into the center of the cylinder. The ends of the slot were fashioned into sharp crack tips using a razor blade. The majority of the specimens were cut so that the longitudinal direction of the sheet stock was in the circumferential direction on the cylinder.

The unsymmetric loading was controlled by the specimen configuration, in that the presence of a stringer introduced the unsymmetric deformations in the region of the crack. In this case the kink angle was obtained directly from the failed specimen.

Computational Aspects

The STAGS computer program has a number of features that are particularly useful in computing the deformations in the vicinity of a crack, and in this project advantage was taken of the ability to easily remove a chosen section of a shell and replace it with a locally refined mesh. In the example shown in Fig. 3 symmetry is assumed about the crack plane, and in this particular case the element size in region 4 is a 0.031-inch square. This symmetric model was also used with the ABAQUS and ANSYS programs. In the unsymmetric case where a stringer is attached the same remeshing approach was used. Examples of this type of grid pattern, as it applies to STAGS, is described by Young et al. [8] for both the symmetric and unsymmetric cases.

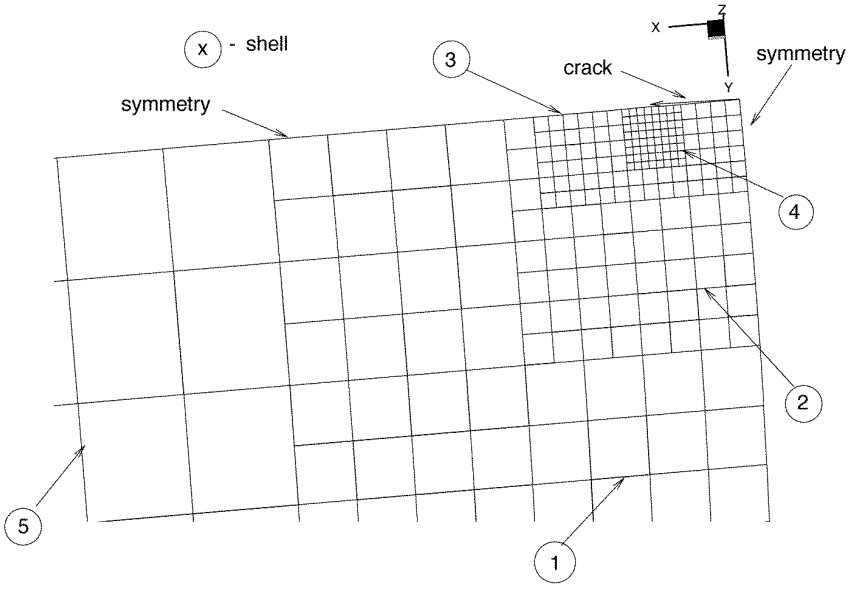

Fig. 3 Symmetric Mesh with Local Remeshing Near the Crack Tip

A finer grid was also generated by halving the distance between the nodes in both the x and y directions, but the results showed little change in the C.M.O.D values, and so the more economical or coarser grid shown in Fig. 3 was used throughout this study.

RESULTS

As the main objective of this study was to use sub scale models to obtain the experimental data to compare with the computational predictions, it had been hoped to study both the experimental and numerical aspects of each configuration simultaneously. However, as this was not always possible the results are presented in terms of the particular deformation being considered, and the numerical results as obtained from STAGS (version 2.0 and 2.3), ABAQUS (version 5.4-1) and ANSYS (version 5.0) are included if they were available.

Bulge Deformations

As the distinguishing feature of an axial crack in a thin cylinder is the bulging, it is appropriate that these deformations should be considered first. Three dimensional views of these deformations were obtained using the "stapl" post-processing capability of STAGS, or by coupling the program output with the TECPLOT [9] data visualization program. An example of this former type of presentation is shown in Fig. 4.

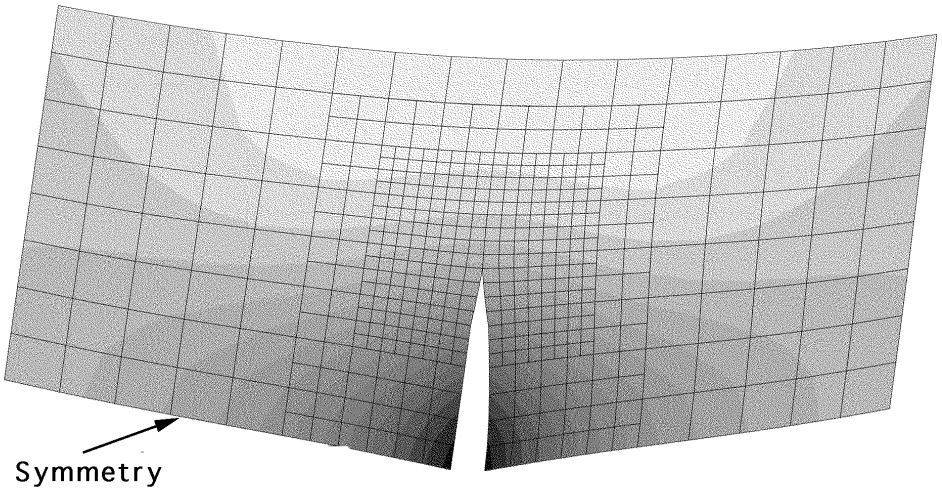

Fig. 4 Radial Displacement Contours in the Vicinity of a Longitudinal Crack

A particular feature of cylinder deformations in the vicinity of an axial crack is the inward deformation or dip ahead of the crack [4]. As can be seen in Figs. 4 and 5 this feature was observed both experimentally and by all three computer codes. As is to be expected, the more ductile 2024-O showed not only larger radial displacements, but also a more

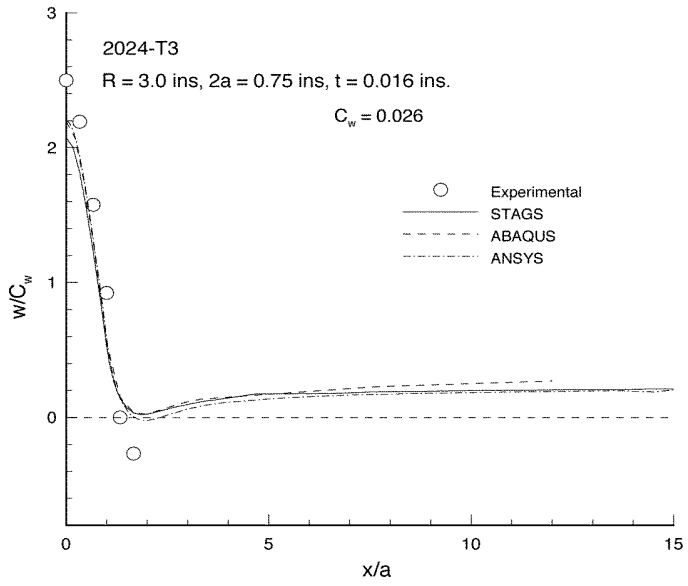

(a)

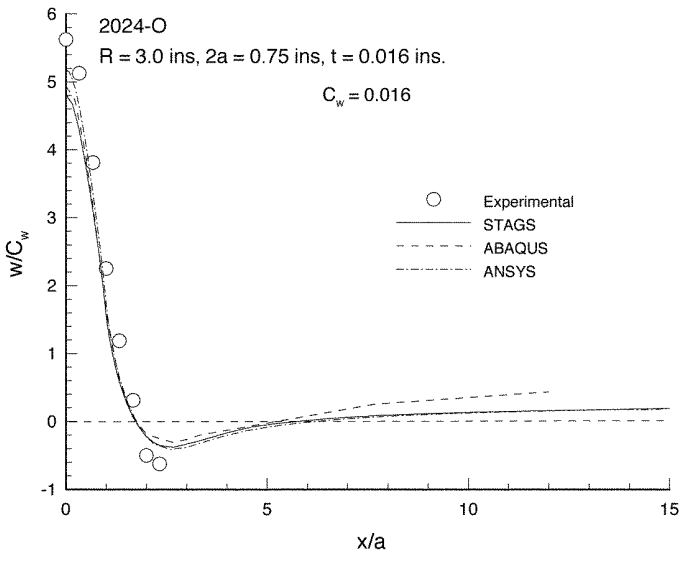

(b)

Fig. 5 Radial Displacements in the Plane of the Crack for a Symmetrically Loaded Thin Cylinder
(a) 2024-T3 at p = 100 psi, (b) 2024-O at p = 60 psi.

pronounced dip. In line with the results reported in [4] the normalizing displacement and crack aspect ratio are

$$C_w = \lambda^2 pR^2/(2Et) \qquad \lambda = [12(1 - \nu^2)]^{1/4} a/\sqrt{(Rt)}$$

The agreement between the experimental and numerical predicted displacements were in general very good. However, near the dip (x/a = 2) and at the center of the crack (x = 0), the experimental values for both cases, were larger than the numerical predicted ones. Although some improvement can be expected using a finer mesh, later studies showed that a more likely cause for the smaller numerical values was due to the fact that no allowance was made for cladding or the small amount of stable crack growth that occurred at these pressures. Also as the experimental values were obtained using the dial gauge system, described earlier, the accuracy of the small deformations measurements associated with the dip might be questioned.

Axial and Hoop strains

In all of the tests the positioning of the strain gauges was largely a matter of individual choice, and so, except for the end conditions described earlier, strain gauges were placed on a point ahead of the projected crack path. In the symmetrically loaded specimens the selected position was in the crack plane, at r = a, while in the stringer experiments the position varied such, that the distance ahead of the crack had value of r equal to a or 2.5a with the angle ahead of the crack varying, depending on the position of the stringer.

The results shown in Figs. 6 through 9 are for the symmetrically loaded cylinders, where it can be seen that all three codes gave comparable results. These experiments, and the corresponding computer analysis, were carried out during the early stages of this project when none of the analysis programs included a stable tearing option. As will be shown later this stable crack growth is an important aspect of thin cylinder failure, and this together with the need to consider the effect of cladding could account for discrepancies between the numerical and experimental results. Unfortunately, it is no longer practical to repeat these analyses and hence eliminate this possible source of error. An interesting feature of these strains is that the axial strains are in tension due to the influence of the bulge. It might also be noted that the axial strain values were measured at a point (x/a = 2) where those strains were changing quite rapidly due to the dip, as shown on Fig. 5, and so a deviation between experiment and predictions might be expected in this case.

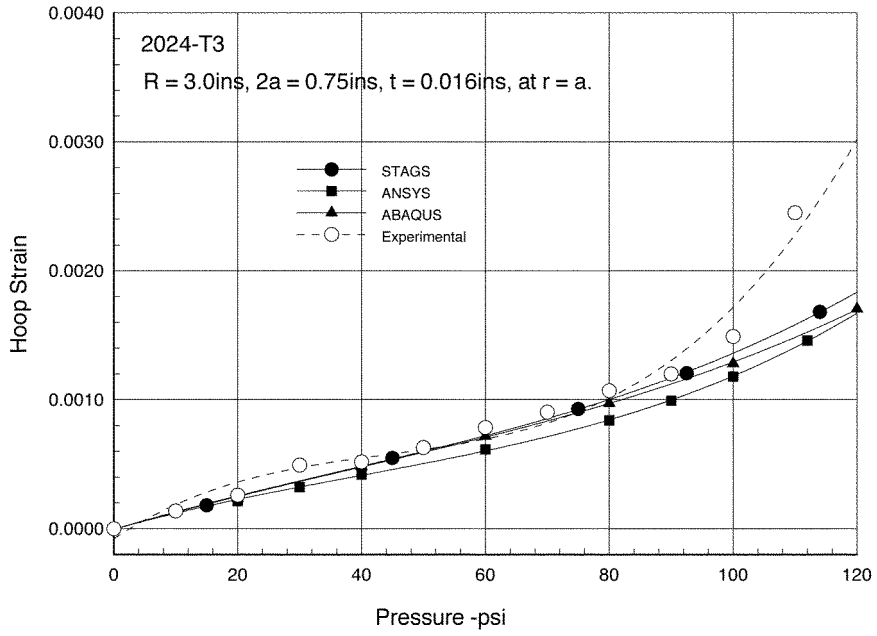

Fig. 6 Hoop Strains at r = a in 2024-T3 Thin Cylinders

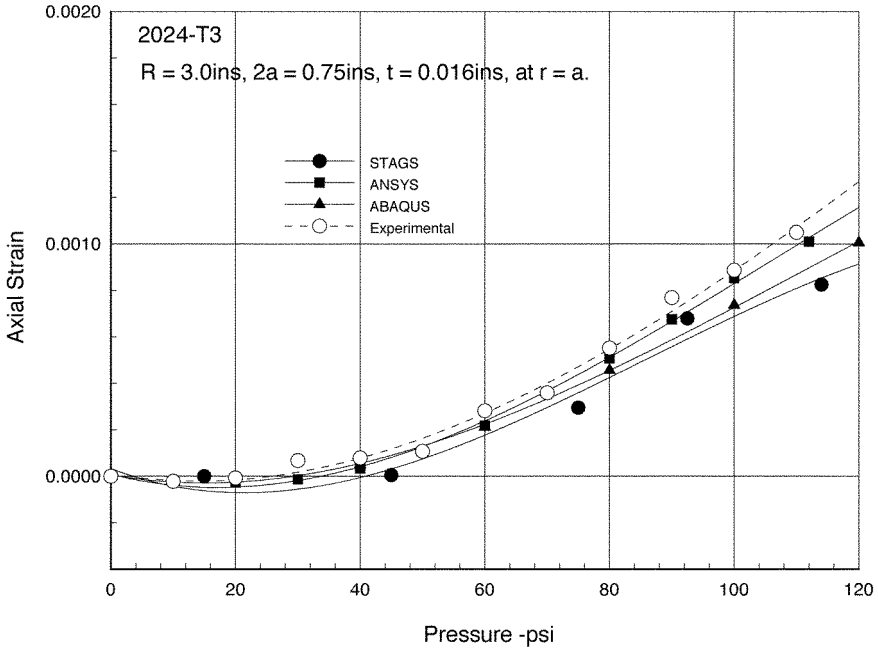

Fig. 7 Axial Strains at r = a in 2024-T3 Thin Cylinders

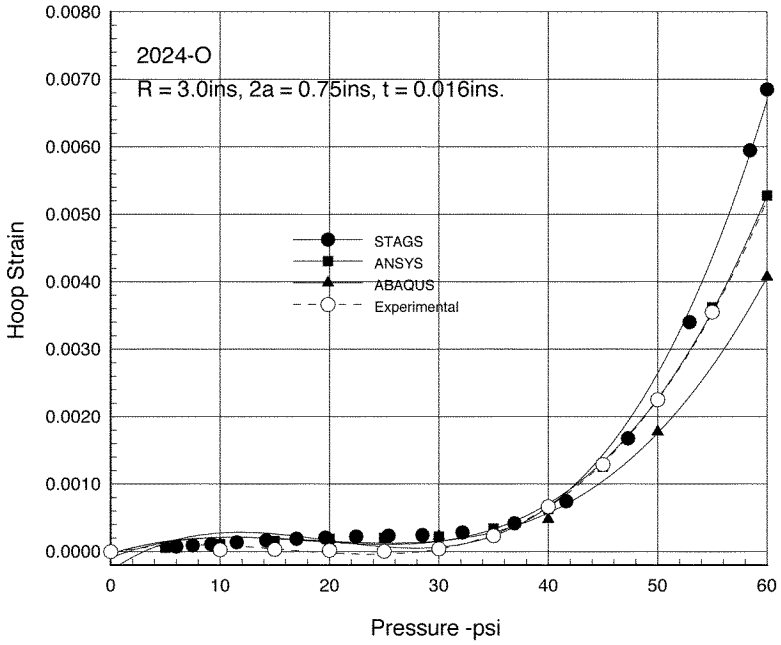

Fig. 8 Hoop Strains at r = a in 2024-O Thin Cylinders

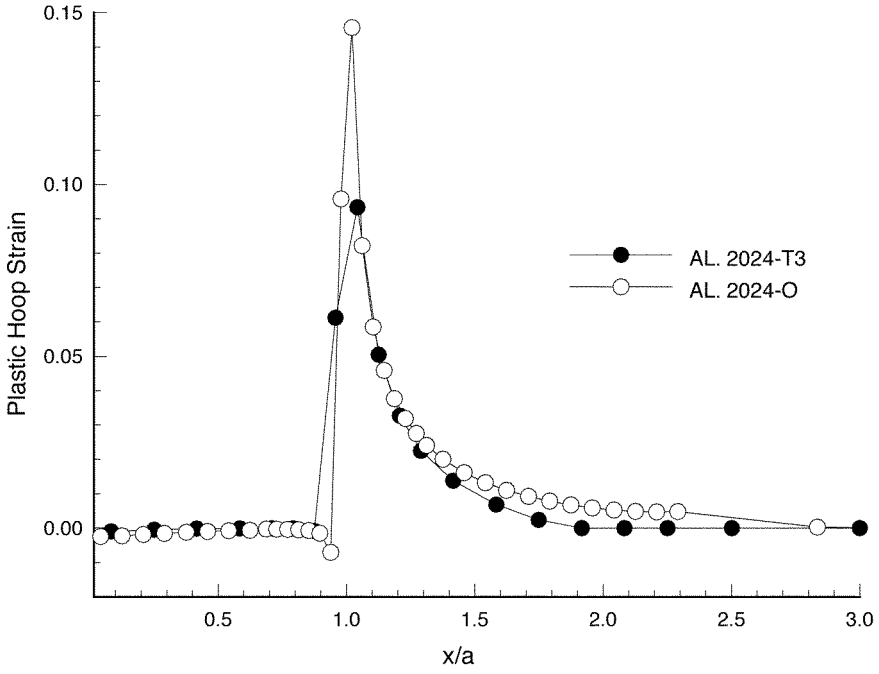

Fig. 9 Crack Tip Plastic Region for 2024-T3 and 2024-O Aluminum Alloys

The results in Fig. 8, where the specimen material was 2024-O, show a much closer agreement between the numerical and experimental results when compared with the higher yield 2024-T3. This feature indicates the importance of the plastic deformations at the crack tip, and could have a significant bearing on how these deformations are modeled in the codes. However, as these results did not allow for either cladding or stable crack growth further analysis is required.

To determine the extent of the plastic region at the crack tip the plastic hoop strains were calculated using the 2.0 version of the STAGS code, and these values are presented in Fig. 9. Clearly any analysis of crack growth, which depends on the deformations in elements at the tip of the crack, requires an accurate determination of these plastic deformations.

The axial strains measured on the edge of the crack at its mid-point (x=0) are not presented in this report as they are essentially linear, but they do indicate that those strains become plastic at the higher pressure levels

Crack Opening Displacements

Crack opening displacements at the center of the crack (C.M.O.D.) were measured in the majority of the cylinders tested, and invariably the experimental displacements appeared to be considerably greater than those initially predicted by STAGS. It can be seen from Figs. 10 and 11, that both ABAQUS and ANSYS also predicted similar values to STAGS. For all three codes the plasticity and large deformation options were used, and the thickness was the nominal value of 0.016 inches. To confirm the experimental results a number of additional tests were conducted using photographic comparisons and direct measurements using calipers. In all cases the experimental values were in general agreement, and considerably larger than those numerically predicted. It is this discrepancy that suggested a low yield material (2024-O) be tested, where the plasticity effects would be emphasized. However, as can be seen in Fig. 11, the low yield material gave closer agreement than the higher yield 2024-T3, which indicated that the particular plasticity models used were not the cause of the discrepancy.

If allowance is made for the cladding the specimen thickness value could be reduced from the nominal 0.016 inches to a nonclad value of 0.0145 inches according to [10], although subsequent measurements of the actual cladding indicated that allowing 0.001 inches for the cladding was more realistic. As can be seen in Fig. 12 this resulted in a closer agreement between the experimental and computed values. This figure also shows that the linear elastic model was clearly inadequate.

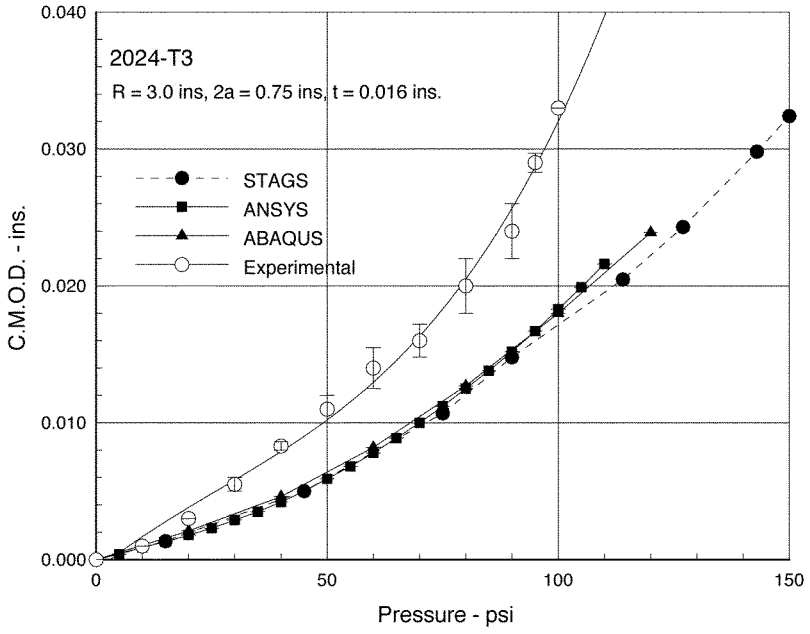

Fig. 10 C.M.O.D. predictions for a 2024-T3 Thin Cylinder

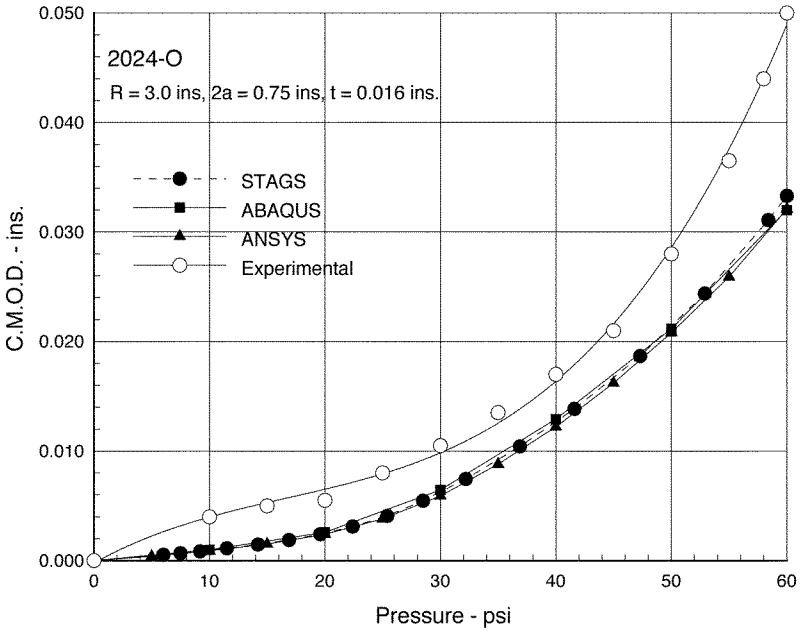

Fig. 11 C.M.O.D predictions for a 2024-O Thin Cylinder

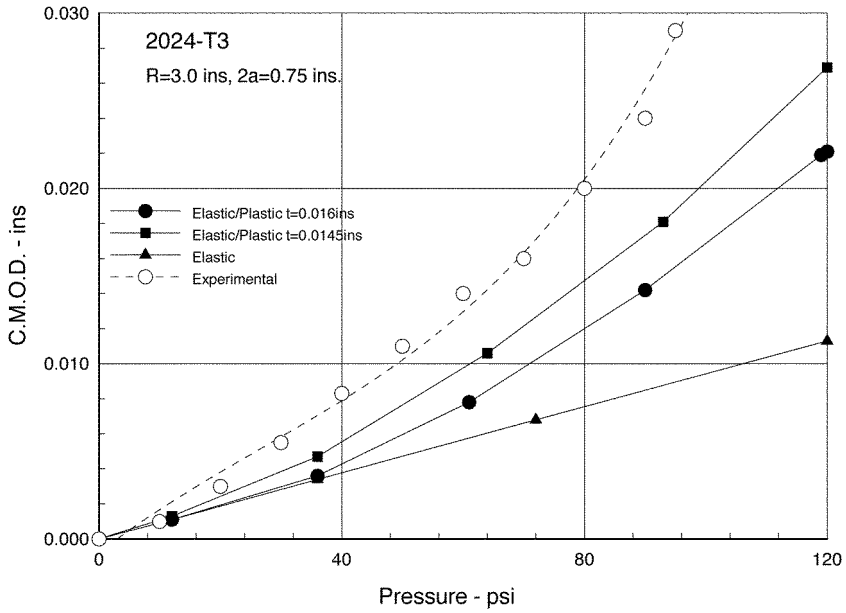

Fig. 12 Influence of Cladding and Plastic deformations on C.M.O.D predictions.

The code inputs were also adjusted to include the loading caused by the polyester seal acting on the edge of the crack, but this additional load provided no significant increase in the predicted displacements.

A close examination of the specimens showed that there was a small, but significant, amount of stable crack growth. This additional crack length was quite small, indeed smaller than the plastic region ahead of the crack.

Crack Tip Opening Angle (C.T.O.A.)

Crack growth prior to failure can be incorporated into the analysis using the stable tearing option available in the 2.3 version of STAGS. However, this option requires that the critical crack tip opening angle be specified as an input parameter, and so a series of tests were conducted in which the crack growth was observed photographically. An example of the results obtained from these tests can be seen in the photograph of Fig. 13, and the C.M.O.D. predictions are presented in Fig. 14. For the configuration under consideration, in which the total specimen thickness was 0.016 inches, the value for the C.T.O.A. was approximately 10^{o}.

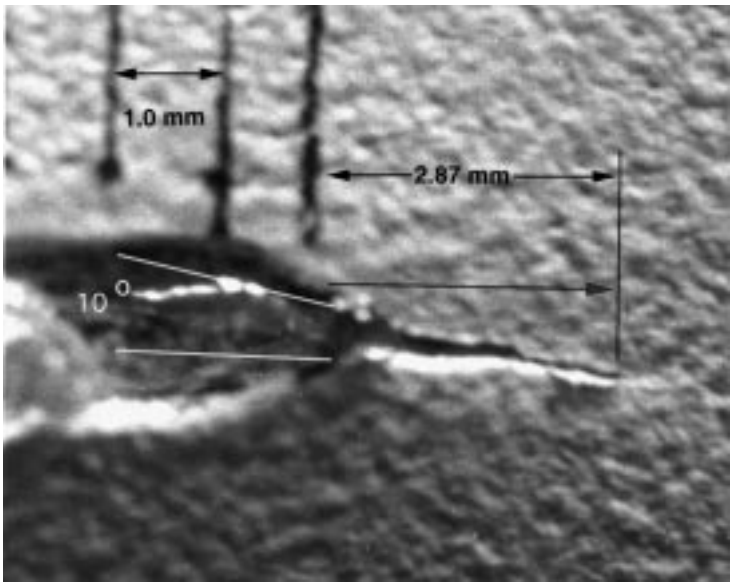

Fig. 13 C.T.O.A. Angle in a Pressurized Specimen just Prior to Failure

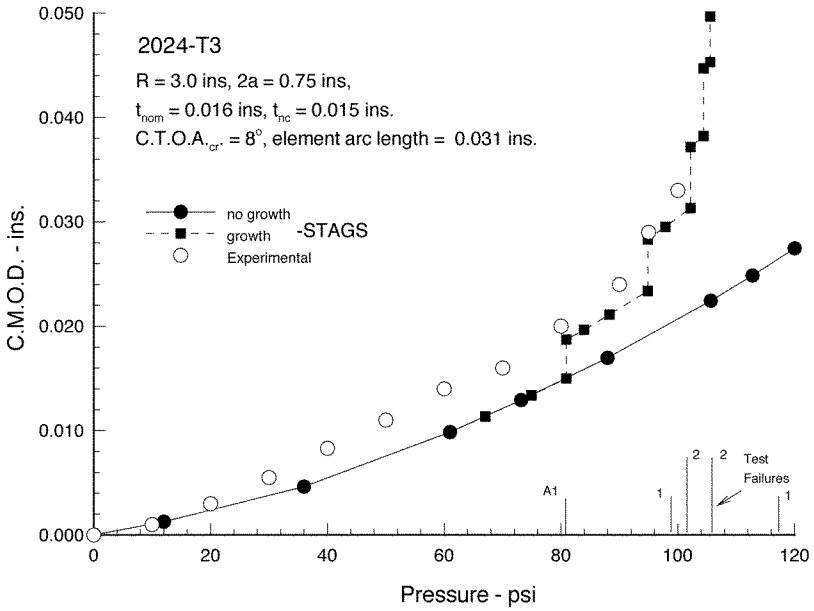

Fig. 14 Influence of Stable Tearing for C.M.O.D. Predictions Using the C.T.O.A. Criterion [11], with A1 the Pressure Measured at Stable Crack Growth Initiation

Although the C.T.O.A. value obtained in these latest tests were approximately 10^{o} it was found that in order to obtain the correct pressure at the onset of stable crack growth, the correct length of this stable crack growth and the final pressure at failure, a critical C.T.O.A. value of 8^{o} was the appropriate value. In these experiments the onset of stable crack growth was defined as the point where the crack had grown by approximately 0.015 inches, which is one half of the finite element grid size used in the region of the crack tip. From Fig. 6 the onset of stable crack growth is also evident by the rapid increase in the hoop strains at that pressure. Clearly the very limited number of tests carried out in which the crack growth was photographed did not allow any idea of how much scatter could be expected in these measurements.

In these additional tests, not only could the pressure at failure be determined, but also the pressure at the onset of stable crack growth, the extent of this growth, and the C.T.O.A. during growth. With this additional knowledge the analysis to obtain C.M.O.D. as a function of applied internal pressure could again be carried out. The improved capability of STAGS in predicting the C.M.O.D values can be seen when the results presented in Fig. 14 are compared with the earlier calculations shown in Fig. 10, this is especially so at the higher pressures just prior to unstable tearing. As mentioned earlier it was felt that the differences at the lower pressures could be due in part to the tendency of the clip gauges to give slightly higher readings as the internal seal acted on the gauge.

A series of tests were conducted in which the crack length was varied, and as can be seen in Fig. 15 the values for both the pressure at failure and the C.M.O.D. changed quite markedly for even modest changes in the crack length. For the tests in which 2a=0.75 ins. the curve in Fig. 15 represent an average (see Appendix). The ability of STAGS to accurately predict these changes was examined where the value of 2a was increased from 0.75 inches to 1.0 inches. The result of this analysis is shown in Fig. 16 where it can be seen that, using the crack tip opening angle criterion, STAGS could be used to predict the onset of stable crack growth and the subsequent cylinder failure.

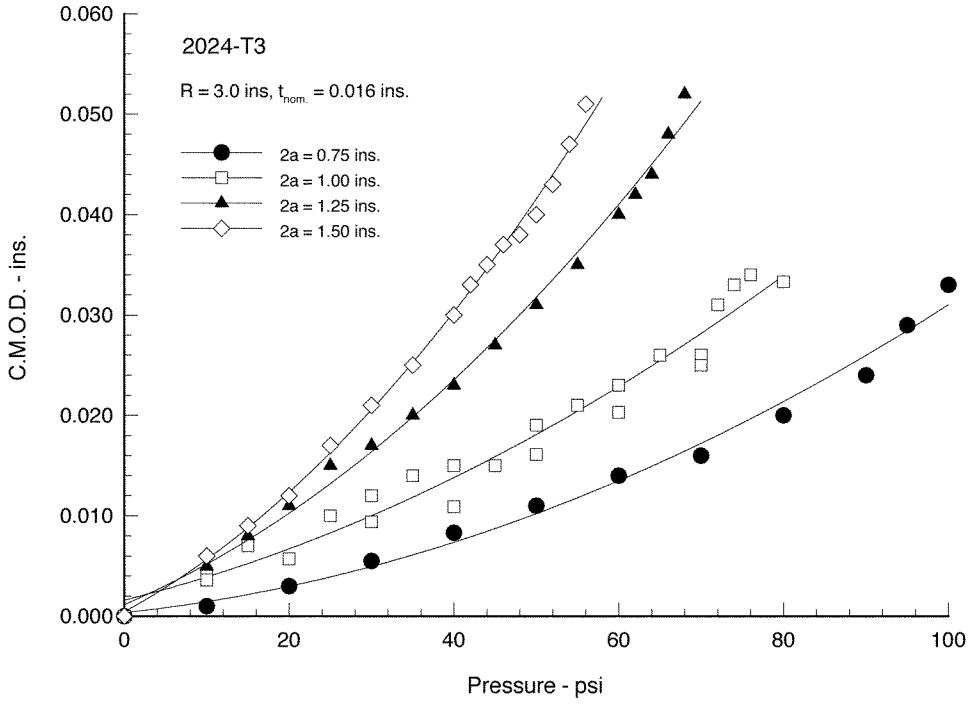

Fig. 15 Experimental measurements of C.M.O.D. for Different Crack Lengths

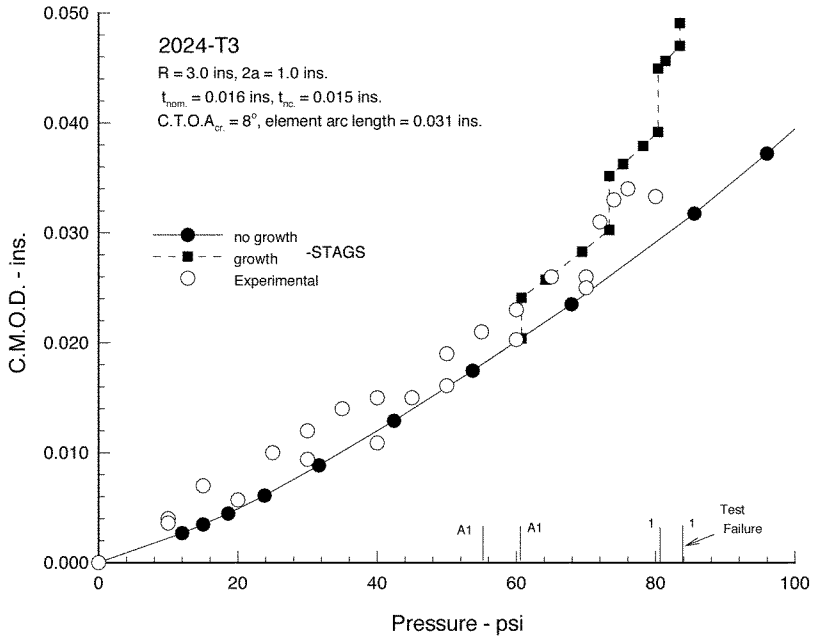

Fig.16 The Variation in C.M.O.D. as a Function of Pressure for 2a= 1.0 inches

Unsymmetric Loading

A number of tests were conducted on cylinders in which the attached stringer created an unsymmetric loading condition. The cylinders in this case were 8 inches in diameter, and of the 2024-T3 material. The stringers were simple 3/8-inch square aluminum rods, which were riveted or epoxyed to the outside of the cylinder, as shown in Fig. 2. In this set of tests the crack no longer extends in the plane of the original crack, but at an angle to this plane. This angle referred to as the kink angle reflects the mixed mode deformations to be expected in the presence of a stringer. Examples of crack growth under mixed mode deformations are shown in Figs. 17. As is to be expected the crack path is controlled by the position of the stringer relative to the crack, and the well defined changes in the kink angle with the distance of the crack from the stringer is a notable feature of the sub scale experiments. However, as this distance is increased it becomes difficult to distinguish between a true kink and the crack curving that also occurs with the unsymmetric loading. Figs. 17a and 17b give examples of crack growth when the stringer was riveted to the cylinder, while Fig. 17c is an example of the case where the stringer had been epoxyed to the cylinder, and in this case the pressure had not quite reached the point of unstable crack growth. In all three cases mode three deformations were observed.

The analysis of this configuration was carried out to determine the kink angle as predicted by STAGS, which used the maximum principal stress criterion [12]. However, as the name of the code implies, the analysis is designed to handle shell structures, and our choice of a stiffener, which was a square rod, could not be readily modeled. However, a reasonable model was obtained by using the discrete stringer option of STAGS. The stringer model in this case was placed on the column that coincided with distance h (see Fig. 18), which is the distance from the crack to the edge of the stringer. As the actual stringer extended over a number of columns, the discrete stringer assumption restricted the region of the STAGS analysis that could be considered as being comparable with the experimental conditions.

In the stringer experiments the strains were also measured at a number of locations ahead of the crack, where it was determined that the influence of the stringer was quite local. This finding was also confirmed by the STAGS analysis, and by the fact that the failure pressure was much higher with the stringer adjacent to the crack, but the stringer had negligible effect when h/a exceeded 3.0. This feature of the influence of the stringer on the failure pressure is shown in Fig. 19.

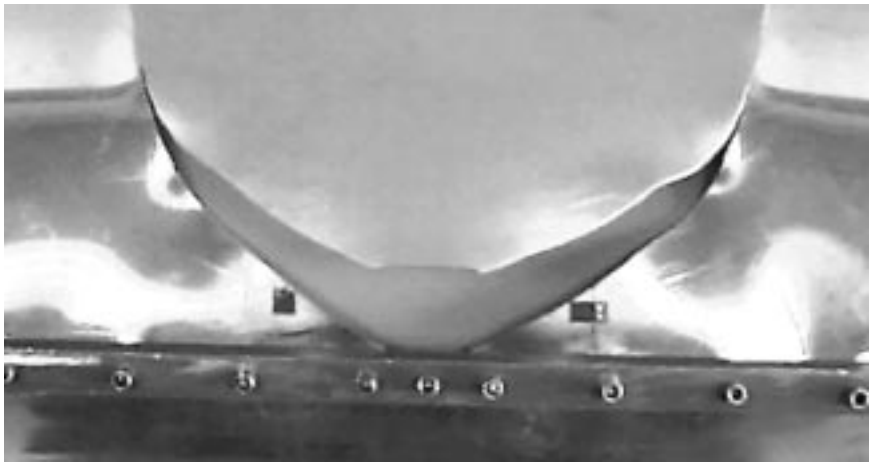

(a)

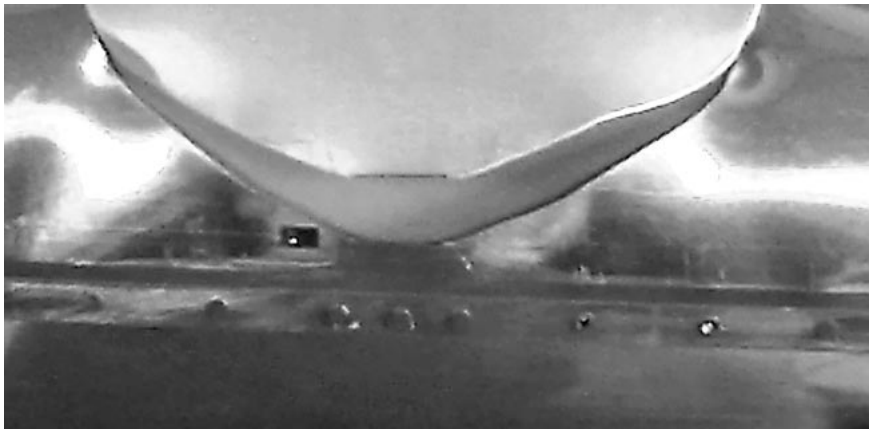

(b)

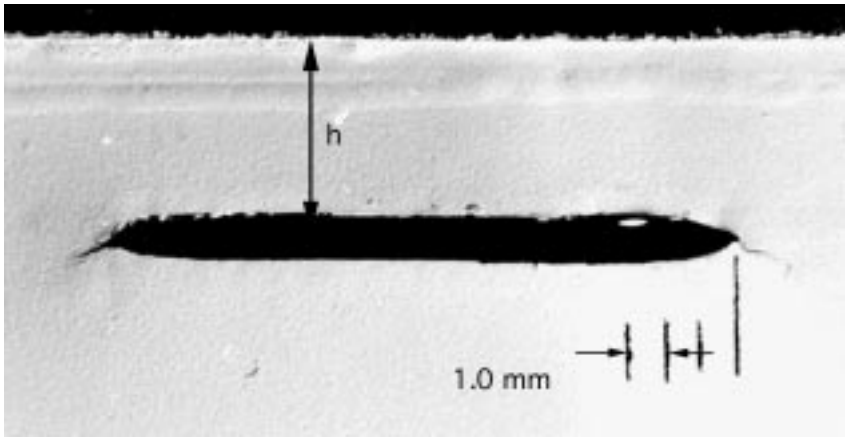

(c)

Fig. 17 Examples of Crack Growth in the Presence of a Stringer

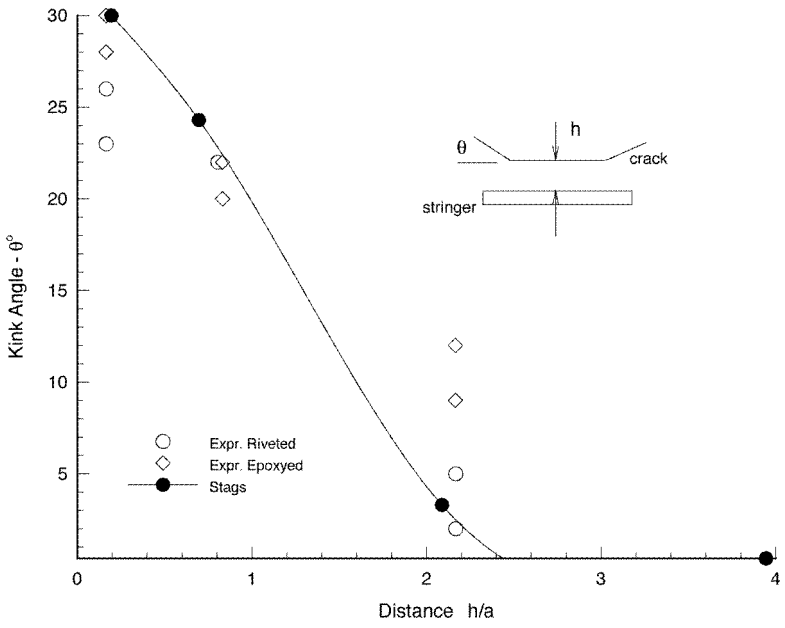

Fig 18 Crack Kinking Angle as a Function of Stringer Location for Parallel Stringers and Cracks

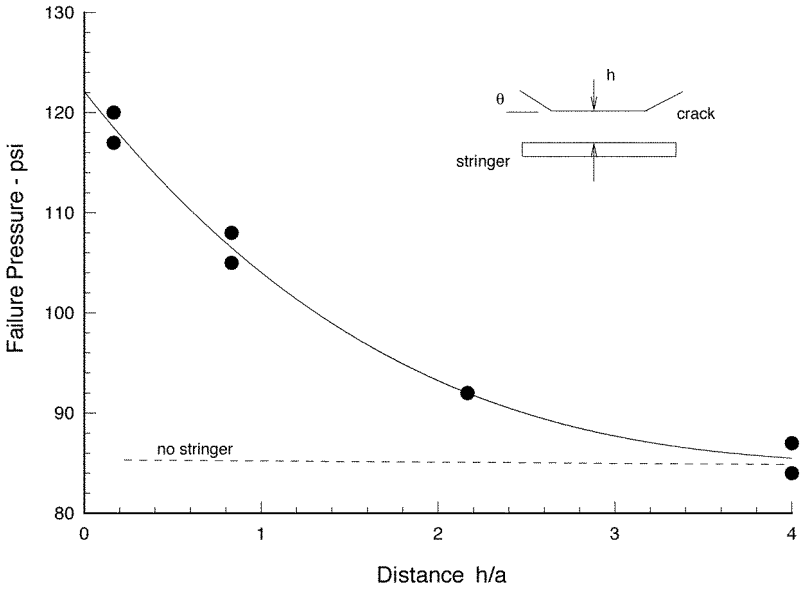

Fig 19 Failure Pressure as a Function of the Distance of Crack from Stringer

The fact that the influence of the stringer is quite local as shown in Figs. 18 and 19 also accounted for the difficulty in measuring the kink angle as the distance between stringer and crack increased. Indeed in these cases the strains obtained in the stringer tests were negligibly different from those obtained in the symmetrically loaded cylinders where the directional instability of the crack growth is due to the presence of the bulge, not the stringer.

CONCLUDING REMARKS

The mixed mode deformations which characterize crack growth in a thin cylindrical shell clearly requires that computer programs designed to provide this analysis should be subjected to extensive experimental verification. The results of this study shows how the sub-scale cylindrical configuration can provide a sufficient variety of tests to provide this model verification at a substantially reduced cost when compared with the full scale counterpart. In particular, it can be seen how the introduction of stable tearing into the analysis greatly improved the predictive capabilities of STAGS, and that the program can predict the deformations associated with the presence of a longitudinal crack in a cylindrical shell with reasonable accuracy.

These tests also highlighted the importance of cladding and the plasticity component in crack analysis; although, in the latter case this may only be in the role of evaluating the particular plasticity model chosen, as it doesn't necessarily follow that plasticity will play such an important role in the full-scale cylinder. However, as plasticity also plays an important role in flat plate analysis it one might assume that it does. An allowance for cladding is clearly required, and as this essentially controls the role played by thickness it should be equally important for the full scale configuration.

The well defined kink angles shown in sub-scale testing provides the data required to further refine and develop the computer models being used to predict crack growth. In this study the crack growth analysis was limited to the initial direction in which the crack would grow, as the complexities introduced by the continual changing direction of subsequent stable crack growth was beyond the scope of the study. It was noted that the closer the crack was to the stringer the higher the required pressure for failure.

These results, when combined with those reported by Fyfe and Sethi [13], show that crack induced bulging can have a significant effect on deformations in the vicinity of the crack. Although, it may be argued that for the large diameters associated with a fuselage, the bulge effect can be ignored and flat plate theory used. However, these studies, together with that of Swift [2], suggest that the influence of the bulging is such, that, even with a large radius cylinder the resultant deformations in the vicinity of a crack may be critically affected in that they can lead to crack curving. In the work of Riks, Brogan and Rankin [14] they indicate that the crack aspect ratio λ is an important measure in the analysis. In a fuselage this number

is typically between 6 and 7 as indicated in the results reported in [7] and so the configuration of the sub-scale models can at least be chosen to meet the requirement of similar values for λ, even though geometric similarity cannot be met.

In general these studies show that the STAGS program provides results which compare very favorably with those provided by ABAQUS and ANSYS. It also shows that, using the C.T.O.A. criterion, STAGS can predict the onset of stable crack growth and the subsequent growth, which eventually leads to the unstable conditions associated with failure.

REFERENCES

[1] Brogan, F. A., Rankin, C. C., and Cabiness, H. D., "STAGS User Manual," Lockheed Palo Alto Research Laboratory, LMSC Report P032594, 1994.

[2] Swift, T., "Damage Tolerance in Pressurized Fuselages," 11th Plantema Memorial Lecture presented to 14th Symposium of the International Committee on Aeronautical Fatigue (ICAF), Ottawa, Canada, June 10-12, 1987.

[3] Folias, E. S. "An Axial Crack in a Pressurized Cylindrical Shell," International Journal of Fracture Mechanics, Vol. 1, No. 2 1965, pp. 104-113.

[4] Erdogan, F. and Ratwani, M., "Fracture of Cylindrical and Spherical Shells Containing a Crack," Nuclear Engineering and Design, Vol. 20, 1972, pp. 265-286.

[5] Zehnder A. T., Viz, M. J. and Ingraffea, A. R., "Fatigue Fracture in Thin Plates Subjected to Tensile and Shearing Loads: Crack Tip Fields, J Integral and Preliminary Experimental Results," Proceedings VII SEM International Congress on Experimental Mechanics, Las Vegas, June 1992.

[6] Potyondy, D. O. and Ingraffea, A. R. "A Methodology for Simulation of Curvilinear Crack Growth in Pressurized Fuselages," Durability of Metal Aircraft Structures, (eds. S. N. Atluri et al.), Atlanta Publ., 1992, pp 167-199.

[7] Miller, M., Kaelber, K. N. and Worden, E. R., "Finite Element Analysis of Pressure Vessel Panels," Durability of Metal Aircraft Structures, (eds. S. N. Atluri et al.), Atlanta Publ., 1992, pp 337-348.

[8] Young, R., Rankin, C., Starnes, J. and Britt, V., "Introduction to Stags", informal report, March 199l.

[9] "Tecplot Version 6 User's Manual," Amtec Engineering, Inc., Bellevue, WA, 1993.

[10] Aluminum Standards & Data, 3rd. Edition, The Aluminum Association, New York, N.Y., 1972.

[11] Newman, J. C. Jr., Bigelow, C. A., and Dawicke, D. S. "Finite-element Analysis and Fracture Simulation in Thin-sheet Aluminum Alloy," Durability of Metal Aircraft Structures, (eds. S. N. Atluri et al.), Atlanta Publ., 1992, pp 167-199.

[12] Erdogan, F. and Sih, G. C., "On the Crack Extension in Plates under Plane Loading and Transverse Shear," J. Basic Eng., 85, 1963, pp. 519-527.

[13] Fyfe, I. M. and Sethi, V. "The Role of Thin Cylinder Bulging on Crack Curvature," AIAA, 32nd Structures, Structural Dynamics, and Materials Conference, Part 2, 1991, pp. 1341-1348.

[14] Riks, E., Brogan, F. A. and Rankin, C. C., "Bulging Cracks in Pressurized Fuselages: A Procedure for Computation," Analytical and Computational Models of Shells, A.K. Noor, T. Belytschko, and J.C. Simo, eds., ASME, New York, ASME CED Vol. 3, 1989, pp. 483-507.

APPENDIX

Summary of Test Program

#of Specimens	Mat'l	Yld, psi	R, in	t , in	2a , in	h, in	#Strain Guages	COD Method	P(f), psi
1	6061-T4	16,000	1.250	0.028	0.75	——	4	Clip, Calip's	375
23	6061-T4	16,000	1.250	0.028	0.75	——	0	Calipers	275-400
2	6061-T4	16,000	1.250	0.028	0.75	——	0	Photos	300-350
Specimen #									
452	2024-T3	44,000	3.000	0.016	——	——	4	——	——
453	2024-T3	44,000	3.000	0.016	0.75	——	4	——	118
457	2024-T3	44,000	3.000	0.016	0.75	——	0	Clip Gauge	105
458	2024-T3	44,000	3.000	0.016	0.75	——	1	——	99
459	2024-T3	44,000	3.000	0.016	0.75	——	4	Clip Gauge	100
480	2024-T3	44,000	3.000	0.016	0.75	——	1	——	——
479 (Tr)	2024-T3	44,000	3.000	0.016	0.75	——	2	Clip Gauge	105
471/483/484	2024-T3	44,000	3.000	0.016	1.00	——	2/0/0	Clip Gauge	84/81/84
472	2024-T3	44,000	3.000	0.016	1.25	——	2	Clip Gauge	70
468	2024-T3	44,000	3.000	0.016	1.50	——	2	Clip Gauge	58
474	2024-T3	44,000	3.000	0.025	0.75	——	2	Clip Gauge	173
475	2024-T3	44,000	3.000	0.025	1.00	——	2	Clip Gauge	139
477	2024-T3	44,000	3.000	0.025	1.25	——	2	Clip Gauge	118
478	2024-T3	44,000	3.000	0.025	1.50	——	2	Clip Gauge	101
460	2024-O	14,000	3.000	0.016	0.75	——	4	Clip Gauge	59
461	2024-O	14,000	3.000	0.016	0.75	——	2	Clip Gauge	62
481	2024-O	14,000	3.000	0.016	0.75	——	1	——	——
462	2024-O	14,000	3.000	0.016	1.50	——	2	Clip Gauge	41
463	2024-T3	44,000	4.000	0.016	0.75	——	4	——	84
464	2024-T3	44,000	4.000	0.016	0.75	——	2	Clip Gauge	87
465	2024-T3	44,000	4.000	0.016	0.75	——	2	Clip Gauge	87
473	2024-T3	44,000	4.000	0.016	1.25	——	2	Clip Gauge	62
476	2024-T3	44,000	4.000	0.016	1.50	——	2	Clip Gauge	53
467	2024-O	14,000	4.000	0.016	0.75	——	2	Clip Gauge	52
466/486	2024-T3	44,000	4.000	0.016	0.75	0.31	2/0	——	108/105
469	2024-T3	44,000	4.000	0.016	0.75	0.81	4	Clip Gauge	92
470/487	2024-T3	44,000	4.000	0.016	0.75	0.06	2/0	Clip Gauge	117/120
490	2024-T3	44,000	3.000	0.016	0.75	0.52	0	U.S.C.	119
491	2024-T3	44,000	3.000	0.016	0.75	0.52	0	U.S.C.	124

REPORT DOCUMENTATION PAGE	Form Approved OMB No. 0704-0188

1. AGENCY USE ONLY (Leave Blank)	2. REPORT DATE	3. REPORT TYPE AND DATES COVERED
	August 1998	Contractor Report

4. TITLE AND SUBTITLE
A Study of Failure in Small Pressurized Cylindrical Shells Containing a Crack

5. FUNDING NUMBERS
WU 538-02-10-01

6. AUTHOR(S)
Craig A. Barwell, Lorenz Eber, and Ian M. Fyfe

7. PERFORMING ORGANIZATION NAME(S) AND ADDRESS(ES)
University of Washington
Seattle, Washington

8. PERFORMING ORGANIZATION REPORT NUMBER

9. SPONSORING/MONITORING AGENCY NAME(S) AND ADDRESS(ES)
National Aeronautics and Space Administration
Washington, DC 20546-0001

10. SPONSORING/MONITORING AGENCY REPORT NUMBER
NASA/CR-1998-208454

11. SUPPLEMENTARY NOTES
Final Report, NASA Contract NAG1-1586, from Professor I. M. Fyfe, Department of Aeronautics and Astronautics, University of Washington, Seattle, WA.

12a. DISTRIBUTION/AVAILABILITY STATEMENT
Unclassified-Unlimited
Subject Category 24 Distribution: Standard
Availability: NASA CASI (301) 621-0390

12b. DISTRIBUTION CODE

13. ABSTRACT (Maximum 200 words)
The deformation in the vicinity of axial cracks in thin pressurized cylinders is examined using small experimental models. The loading applied was either symmetric or unsymmetric about the crack plane, the latter being caused by structural constraints such as stringers. The objective was two fold - one, to provide the experimental results which will allow computer modeling techniques to be evaluated for deformations that are significantly different from that experienced by flat plates, and the other to examine the deformations and conditions associated with the onset of crack kinking which often precedes crack curving.

The stresses which control crack growth in a cylindrical geometry depend on conditions introduced by the axial bulging, which is an integral part of this type of failure. For the symmetric geometry, both the hoop and radial strain just ahead off the crack, r = a, were measured and these results compared with those obtained from a variety of structural analysis codes, in particular STAGS [1], ABAQUS and ANSYS. In addition to these measurements, the pressures at the onset of stable and unstable crack growth were obtained and the corresponding crack deformations measured as the pressures were increased to failure. For the unsymmetric cases, measurements were taken of the crack kinking angle, and the displacements in the vicinity of the crack.

In general, the strains ahead of the crack showed good agreement between the three computer codes and between the codes and the experiments. In the case of crack behavior, it was determined that modeling stable tearing with a crack-tip opening displacement fracture criterion could be successfully combined with the finite-element analysis techniques as used in structural analysis codes. The analytic results obtained in this study were very compatible with the experimental observations of crack growth. Measured crack kinking angles also showed good agreement with theories based on the maximum principle stress criterion.

14. SUBJECT TERMS
Fracture; CTOA; STAGS; Cylinders; Cracks; Plasticity

15. NUMBER OF PAGES
34

16. PRICE CODE
A03

17. SECURITY CLASSIFICATION OF REPORT	18. SECURITY CLASSIFICATION OF THIS PAGE	19. SECURITY CLASSIFICATION OF ABSTRACT	20. LIMITATION OF ABSTRACT
Unclassified	Unclassified	Unclassified	